ANL-6937

ANL-6937

Argonne National Laboratory

A STUDY OF UNSTEADY MAGNETOHYDRODYNAMIC FLOW AND HEAT TRANSFER

by

Ralph M. Singer

Printed in USA. Price $2.00. Available from the Clearinghouse for Federal Scientific and Technical Information, National Bureau of Standards, U. S. Department of Commerce, Springfield, Virginia

ANL-6937
Propulsion Systems and
Energy Conversion
(TID-4500, 37th Ed.)
AEC Research and
Development Report

ARGONNE NATIONAL LABORATORY
9700 South Cass Avenue
Argonne, Illinois 60440

A STUDY OF UNSTEADY MAGNETOHYDRODYNAMIC FLOW AND HEAT TRANSFER

by

Ralph M. Singer

Reactor Engineering Division

November 1964

Operated by The University of Chicago
under
Contract W-31-109-eng-38
with the
U. S. Atomic Energy Commission

TABLE OF CONTENTS

LIST OF FIGURES

LIST OF TABLES

o

NOTATION

English Letters

a	One-half of channel wall separation
A	Gradient of wall temperature in x-direction
B	Dimensionless induced magnetic field, $B = B_x/B_0$
B_0	Applied magnetic field
$\underline{B}$	Magnetic induction vector
B_m	Transformed value of B (Fourier)
$\overline{B}_m$	Transformed value of B (Fourier and Laplace)
c	Heat capacity
$F, F(Y,\tau)$	Dimensionless internal-energy generation rate, aQ/kA
F_m	Transformed value of F (Fourier)
$\overline{F}_m$	Transformed value of F (Fourier and Laplace)
$\underline{g}$	Gravitational acceleration vector
$G, G(\tau)$	Dimensionless pressure-gradient term, $(a^3/\mu\alpha)(-\frac{\partial p}{\partial x} - \rho g)$
G_m	Transformed value of G (Fourier)
$\overline{G}_m$	Transformed value of G (Fourier and Laplace)
$H, H(\tau)$	Dimensionless time derivative of wall temperature, $(a/\alpha A)(\partial T_w/\partial t)$
H_m	Transformed value of H (Fourier)
$\overline{H}_m$	Transformed value of H (Fourier and Laplace)
m	Fourier summation index
M	Hartmann number, $B_0 a(\sigma/\mu)^{1/2}$
P_r	Thermal Prandtl number, ν/α
Pr_m	Magnetic Prandtl number, $\nu/\nu_m = \mu_0\sigma\nu$
p	Pressure
q	Heat flux
Q	Volumetric Internal-energy generation rate
Ra	Rayleigh number, $g\beta a^4 APr/\nu^2$
s	Laplace variable
t	Time
T	Temperature
u	Velocity in x-direction
U	Dimensionless velocity in x-direction, $U = au/\alpha$
U_m	Transformed value of U (Fourier)
$\overline{U}_m$	Transformed value of U (Fourier and Laplace)
$\underline{V}$	Velocity vector
x,y	Linear coordinates
Y	Dimensionless form of y, $Y = y/a$

Greek Letters

α	Thermal diffusivity
β	Coefficient of thermal expansion
γ	Function defined in second footnote on page 12
θ	Dimensionless temperature difference, $\theta = (T - T_w)/aA$
θ_m	Transformed value of θ (Fourier)
$\overline{\theta}_m$	Transformed value of θ (Fourier and Laplace)
μ	Dynamic viscosity
μ_0	Magnetic permeability
ν	Kinematic viscosity, μ/ρ
ν_m	Magnetic diffusivity, $(\sigma\mu_0)^{-1}$
ρ	Density
σ	Electrical conductivity
τ	Dimensionless time, $\tau = \alpha t/a^2$
$\psi_j(m,\tau)$	Functions defined in Appendix C

Subscripts

f	Fluid conditions
i	Initial conditions
M	Mean value
MM	Mixed-mean value
R	Reference temperature
ss	Steady-state condition
W	Wall conditions
x	Component of vector in x-direction

A STUDY OF UNSTEADY MAGNETOHYDRODYNAMIC FLOW AND HEAT TRANSFER

by

Ralph M. Singer

ABSTRACT

The unsteady, combined free and forced convective flow of an electrically conducting fluid through a transverse magnetic field is analyzed. Allowing the channel wall temperature to vary linearly with the axial coordinate of the duct allows a fully-developed flow situation that linearizes the governing equations and permits an analytical solution. The unsteadiness may occur because of variations in the axial pressure gradient, wall temperature, or internal energy generation rate. The effects of the thermal and magnetic Prandtl numbers (Pr and Pr_m), the Hartmann number (M), the Rayleigh number (Ra), and internal energy generation upon the flow and heat transfer is studied. Oscillatory behavior is observed for large values of Ra and M and for Pr near unity, and the length of the transient period is found to depend strongly upon these parameters.

INTRODUCTION

In recent years, considerable interest has developed in magnetohydrodynamic channel flow because of its application to energy conversion schemes, e.g., power generators, electromagnetic pumps, and flow meters. Although a wealth of information exists on the steady, laminar flow of an electrically conducting fluid through a channel in the presence of a transverse magnetic field (e.g., References 1, 2, 3, 4), only a few studies are available that deal with unsteady MHD channel flow. Results of such studies are of interest in the design of MHD devices because of possible instabilities or overheating that may occur during start-up or shut-down.

Unsteady MHD flows across flat plates are analyzed in several papers, but these papers will not be discussed here and attention is restricted to equivalent channel-flow problems. To this author's knowledge, the earliest work of this kind was presented by Chekmarev[5] who considered a parallel-plate channel with infinitely thick, electrically conducting walls, and an initial applied magnetic field. At zero time, a constant pressure gradient is applied and the fluid is set in motion. Unfortunately, no numerical results were presented.

The case of a parallel-plate channel with walls of infinite electrical conductivity and a suddenly applied constant magnetic field, coupled with either a step, step-periodic, or impulsive change in the pressure gradient, was studied by Yen and Chang(6). Their results were limited to only a few sets of the physical parameters, and therefore the oscillatory approach to steady-state conditions which can occur, was not observed. This paper was extended by Tao(7) who indicated the existence of flow oscillations when the magnetic Prandtl number was near unity. In Tao's brief note, only limited numerical data were presented, and the effects of the Hartmann and magnetic Prandtl numbers were not fully discussed.

This same problem was again solved by Ogawa and Sone(8) by an alternative mathematical technique, and results were presented only for the very special case of the viscous and magnetic Reynold's numbers and a pressure number equal to unity.

The transient flow of an electrically conducting fluid in a tube of arbitrary cross section situated in a magnetic field following a step-change in the axial pressure gradient was treated by Uflyand(9). The general results were specialized to the cases of rectangular and circular cross sections, but no numerical data were presented.

In the aforementioned papers, only isothermal flow was considered. To the author's knowledge, no results exist for unsteady, convective MHD channel flow. Several papers do exist, however, that deal with unsteady, convective channel flow in the absence of a magnetic field. In combined forced and natural convection, Zeiberg and Mueller(10) found that an oscillatory approach to steady-state conditions following a step change in the wall temperature can occur. The amplitude and frequency of these oscillations (which occur both in the velocity and temperature) increase as the Rayleigh number increases. The effect of the thermal Prandtl number on the transient phenomena was also indicated for values of Pr from 0.01 to 100.

Tao(11) considered a similar problem to that in (10), except a circular tube was used and a different mathematical approach was utilized. Again, damped oscillations in the velocity were observed at large values of the Rayleigh number following a change in the axial pressure gradient.

Apparently, the transient, combined forced and natural convective channel flow of an electrically conducting fluid in a transverse magnetic field has not been studied. This problem is of interest in the ultimate design of an MHD power generator because of possible electrical overloading during the oscillatory transient period in start-up or shut-down.* Also, since in all such generators, an extremely hot fluid (e.g., liquid sodium at 1200°F) will be used, the problem of heat transfer from the fluid to the channel walls would be important.

* Since the power output from an MHD generator is proportional to the square of the mean flow velocity, velocity oscillations can cause large power oscillations.

In this paper, the unsteady, combined convective flow of an electrically conducting fluid through a vertical, parallel-plate channel in a horizontal magnetic field will be considered. Unsteadiness can be caused by prescribed variations in the axial pressure gradient and/or the wall temperature. The flow and heat transfer will be assumed to be fully developed, and the conditions under which this assumption is valid will be indicated. This assumption, along with that of perfect electrically conducting walls, leads to a system of linear partial differential equations which are amenable to Fourier and Laplace transformations.

MATHEMATICAL FORMULATION

The energy and MHD equations (in mks units) for incompressible, nondissipative, viscous flow are (12)

$$\frac{\partial \underline{B}}{\partial t} = \nabla \times (\underline{V} \times \underline{B}) + \nu_m \nabla^2 \underline{B}, \tag{1}$$

$$\nabla \cdot \underline{V} = 0, \tag{2}$$

$$\rho \left[\frac{\partial \underline{V}}{\partial t} + (\underline{V} \cdot \nabla)\underline{V} \right] = -\nabla p + \mu \nabla^2 \underline{V} + \frac{1}{\mu_0}(\nabla \times \underline{B}) \times \underline{B} + \rho \underline{g}, \tag{3}$$

and

$$\frac{\partial T}{\partial t} + \underline{V} \cdot \nabla T = \alpha \nabla^2 T + \frac{Q}{\rho c}, \tag{4}$$

where it has been assumed that no excess charges are present and the displacement current and viscous and ohmic dissipation are negligible. Also, all physical properties (except the density in the formulation of the buoyancy term) are assumed to be isotropic and constant.

For nonsteady, fully developed flow and heat transfer, it can be shown that $\underline{V} = [u(y,t), 0, 0]$ and $\underline{B} = [B_x(y,t), B_0, 0]$, (see Reference 6), so that equations (1) through (4) reduce to (the coordinate system is shown in Figure 1)

$$\frac{\partial B_x}{\partial t} = B_0 \frac{\partial u}{\partial y} + \nu_m \frac{\partial^2 B_x}{\partial y^2}, \tag{5}$$

$$\rho_R \frac{\partial u}{\partial t} = - \frac{\partial p}{\partial x} + \mu_R \frac{\partial^2 u}{\partial y^2} + \frac{B_0}{\mu_0} \frac{\partial B_x}{\partial y} - \rho_R g \,[1 - \beta\,(T - T_R)], \tag{6}$$

$$0 = -\frac{\partial \rho}{\partial y} - \frac{B_x}{\mu_0}\frac{\partial B_x}{\partial y}, \tag{7}$$

and

$$\frac{\partial T}{\partial t} + u\frac{\partial T}{\partial x} = \alpha_R\left(\frac{\partial^2 T}{\partial x^2} + \frac{\partial^2 T}{\partial y^2}\right) + \frac{Q}{\rho_R c_R}, \tag{8}$$

where the subscript R refers to a reference temperature, and the buoyancy term in equation (6) came from the assumption

$$\rho = \rho_R\,[1 - \beta(T - T_R)]. \tag{9}$$

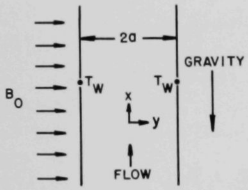

Fig. 1
Physical Model and Coordinate System

112-4417

The determination of the functional form of the temperature field that will allow a fully developed unsteady flow in the pressure of a magnetic field is shown in Appendix A.

From the arguments in Appendix A, the governing equations for unsteady, fully developed MHD flow may be written in dimensionless flow as follows:

$$\frac{\partial B}{\partial \tau} = \frac{\partial U}{\partial Y} + \left(\frac{Pr}{Pr_m}\right)\frac{\partial^2 B}{\partial Y^2}, \tag{10}$$

$$\frac{1}{Pr}\frac{\partial U}{\partial \tau} = \frac{\partial^2 U}{\partial Y^2} + \left(\frac{M^2 Pr}{Pr_m}\right)\frac{\partial B}{\partial Y} + Ra\theta + G(\tau), \tag{11}$$

and

$$\frac{\partial \theta}{\partial \tau} = \frac{\partial^2 \theta}{\partial Y^2} - U + F(Y,\tau) - H(\tau), \tag{12}$$

where Pr is the thermal Prandtl number, Pr_m the magnetic Prandtl number, M the Hartmann number, Ra the Rayleigh number, $G(\tau)$ a pressure gradient term, $H(\tau)$ a wall temperature gradient term, and $F(Y,\tau)$ an internal energy generation index.*

To specify the initial and boundary conditions, the following situation is analyzed.

Initially, for $\tau < 0$, some steady distribution of velocity, temperature, and induced magnetic field exists; i.e.,

$$U(Y,0) = U_i(Y),$$

$$\theta(Y,0) = \theta_i(Y), \tag{13}$$

and

$$B(Y,0) = B_i(Y),$$

and for subsequent time, $\tau > 0$, the forced-convection pressure gradient, wall temperature, and internal energy generation rate vary arbitrarily with time. With no loss of generality, the boundary conditions are taken as

$$U(\pm 1,\tau) = 0,$$

$$\theta(\pm 1,\tau) = 0, \tag{14}$$

and

$$\frac{\partial B(\pm 1,\tau)}{\partial Y} = 0,$$

which requires both channel walls to have equal temperatures at any height for all time and requires the walls to be perfect electrical conductors [relative to the fluid; see (4)].

The detailed mathematics involved in the solution of equations (10), (11), and (12) with conditions (13) and (14) are presented in Appendix B.

---

*See the Notation for definitions.

STEP CHANGE IN PRESSURE GRADIENT AND WALL TEMPERATURE

Consider the following situation: Initially there is no flow (zero pressure gradient) and no heat transfer (the temperatures of the fluid and the wall are both equal to some constant value, say T_0). Suddenly, a constant pressure gradient is impressed in the x-direction, the wall temperature is increased to some constant (in time) level above the fluid temperature (the gradient of the wall temperature in the x-direction is also fixed at some constant level, A, or equivalently, the wall heat flux is fixed at some constant value, q_w), and the fluid starts to generate heat at a uniform rate. From the definitions of $F(Y,\tau)$, $G(\tau)$, and $H(\tau)$, it is seen that F and G are constant and H is zero for $\tau > 0$. Also, $B_{mi} = U_{mi} = \theta_{mi} = 0$.

Thus, the convolution integrals in the appendices can be explicitly evaluated, and the following expressions for $U(Y,\tau)$, $\theta(Y,\tau)$, and $B(Y,\tau)$ can be found for the cases of $(Pr/Pr_m) = 1$ and $(Pr/Pr_m) \gg 1$:*

$$U(Y,\tau) = \sum_{\gamma^2<0}\left[\frac{G_m\psi_1(m,\tau) + RaF_m\psi_2(m,\tau)}{\left(\frac{m\pi}{2}\right)^4 + M^2\left(\frac{m\pi}{2}\right)^2 + Ra}\right]\sin\left[\frac{m\pi}{2}(Y+1)\right] + \psi_3(m_0,\tau)\sin\left[\frac{m_0\pi}{2}(Y+1)\right]$$

$$+\sum_{\gamma^2>0}\left[\frac{G_m\psi_4(m,\tau) + RaF_m\psi_5(m,\tau)}{\left(\frac{m\pi}{2}\right)^4 + M^2\left(\frac{m\pi}{2}\right)^2 + Ra}\right]\sin\left[\frac{m\pi}{2}(Y+1)\right], \qquad (15)^{**}$$

$$-\theta(Y,\tau) = \sum_{\gamma^2<0}\left[\frac{G_m\psi_2(m,\tau) + RaF_m\psi_6(m,\tau)}{\left(\frac{m\pi}{2}\right)^4 + M^2\left(\frac{m\pi}{2}\right)^2 + Ra}\right]\sin\left[\frac{m\pi}{2}(Y+1)\right] + \psi_7(m_0,\tau)\sin\left[\frac{m_0\pi}{2}(Y+1)\right]$$

$$+\sum_{\gamma^2>0}\left[\frac{G_m\psi_5(m,\tau) + RaF_m\psi_8(m,\tau)}{\left(\frac{m\pi}{2}\right)^4 + M^2\left(\frac{m\pi}{2}\right)^2 + Ra}\right]\sin\left[\frac{m\pi}{2}(Y+1)\right]$$

$$-\sum_{m=1}^{\infty} F_m\left(\frac{2}{m\pi}\right)^2\left[1 - e^{-\left(\frac{m\pi}{2}\right)^2\tau}\right]\sin\left[\frac{m\pi}{2}(Y+1)\right], \qquad (16)$$

---

*Since the solutions for the two cases are similar, an abbreviated notation will be used wherein the functions $\psi_i(m,\tau)$ will be tabulated according to the value of Pr/Pr_m.

**For $Pr/Pr_m = 1$, $\gamma^2 \equiv (m\pi/2)^4(1-Pr)^2 - 4M^2(m\pi/2)^2 Pr - 4RaPr$; while for $(Pr/Pr_m) \gg 1$, $\gamma^2 \equiv (m\pi/2)^4(1-Pr)^2 - 2M^2(m\pi/2)^2Pr(1-Pr) + M^4Pr^2 - 4RaPr$. Also, the symbol $\sum_{\gamma^2<0}$ is meant to represent a summation over all values of m such that $\gamma^2 < 0$. A similar meaning is imposed on $\sum_{\gamma^2>0}$. The term m_0 is the value of m such that $\gamma^2 = 0$.

and

$$B(Y,\tau) = \sum_{\gamma^2<0} \left[\frac{G_m \psi_9(m,\tau) + RaF_m \psi_{10}(m,\tau)}{\left(\frac{m\pi}{2}\right)^4 + M^2\left(\frac{m\pi}{2}\right)^2 + Ra} \right] \left(\frac{m\pi}{2}\right) \cos\left[\frac{m\pi}{2}(Y+1)\right]$$

$$+ \left(\frac{m_0\pi}{2}\right) \psi_{11}(m_0,\tau) \cos\left[\frac{m_0\pi}{2}(Y+1)\right]$$

$$+ \sum_{\gamma^2>0} \left[\frac{G_m \psi_{12}(m,\tau) + RaF_m \psi_{13}(m,\tau)}{\left(\frac{m\pi}{2}\right)^4 + M^2\left(\frac{m\pi}{2}\right)^2 + Ra} \right] \left(\frac{m\pi}{2}\right) \cos\left[\frac{m\pi}{2}(Y+1)\right], \quad (17)$$

where the functions $\psi_i(m,\tau)$ are defined in Appendix C.

From equations (15) and (16), average values of the velocity and temperature difference functions can be calculated, using the definitions

$$U_M(\tau) = \frac{1}{2} \int_{-1}^{+1} U(Y,\tau) dY, \quad (18)$$

$$\theta_M(\tau) = \frac{1}{2} \int_{-1}^{+1} \theta(Y,\tau) dY, \quad (19)$$

and

$$\theta_{MM}(\tau) = \frac{1}{2U_M(\tau)} \int_{-1}^{+1} U(Y,\tau)\theta(Y,\tau) dY, \quad (20)$$

where $\theta_{MM}(\tau)$ is the mixed-mean temperature difference function. The results of carrying out the integrations indicated in equations (18), (19), and (20) are shown in Appendix D.

Finally, Nusselt numbers can be defined based on either the mean temperature difference or the mixed-mean temperature difference. The standard definition for Nu is

$$Nu = \frac{h \cdot 2a}{k} = \frac{q_W \cdot 2a}{k(T_W - T_f)}, \quad (21)$$

where the subscript W refers to the wall and f to the fluid. The wall heat flux, q_W, can be related to the axial temperature gradient, A, and the heat generation rate by a simple overall energy balance,

$$q_W = a(\rho c u_M A - Q), \tag{22}$$

where u_M is the mean velocity. Substitution of (22) into (21), and using the definitions of the dimensionless quantities, results in

$$Nu = \frac{2(F - U_M)}{\theta_f}, \qquad \theta_f = (T_f - T_W)/aA. \tag{23}$$

Thus, the quantities Nu_M and Nu_{MM} can be defined as

$$Nu_M = 2(F - U_M)/\theta_M, \tag{23a}$$

and

$$Nu_{MM} = 2(F - U_M)/\theta_{MM}. \tag{23b}$$

RESULTS AND DISCUSSION

Effects of the Hartmann Number

The effects of the Hartmann number (essentially a measure of the magnetic body force relative to the viscous force) upon the dimensionless mean velocity and temperature functions and the Nusselt number are shown in Figures 2, 4, and 5, respectively. The velocity shown in these figures is U_M/G, or in terms of physical quantities, $(\mu u_M/a^2)/\left(-\frac{\partial p}{\partial x} - \rho g\right)$.

In Figure 2, the curve labeled $M = 0$ represents the following situation: Initially the fluid is motionless and at a uniform temperature;

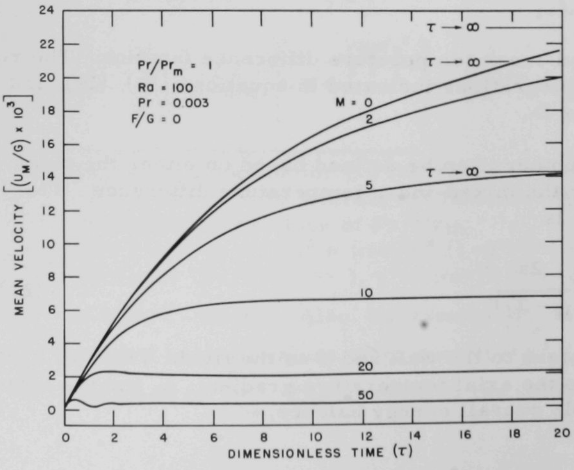

Fig. 2

Effect of Hartmann Number on Transient Mean Velocity at zero time, the pressure gradient is suddenly increased to some constant level, and the wall temperature is changed a negligible amount. The fluid is then set into motion, and the velocity asymptotically approaches a steady value at some time $\tau > 20$. The curves labeled M = 2, 5, 10, 20, and 50 represent situations in which an external magnetic field is instantaneously turned on, along with the pressure gradient change. Since $Pr/Pr_m = 1$ in this figure (relatively small value of the magnetic diffusivity), the magnetic field is delayed in its penetration of the fluid, and as a result, and overshoot and oscillation is observed for M greater than about 20.

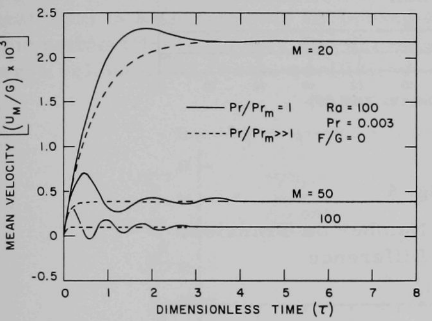

112-4416

Fig. 3

Effect of Magnetic Prandtl Number on Transient Mean Velocity

This oscillation can be eliminated entirely if $Pr/Pr_m \gg 1$ (very large magnetic diffusivity) as shown in Figure 3. The solid lines indicate the situations in which the magnetic field and pressure gradient are simultaneously changed and the fluid has a small magnetic diffusivity; the dashed lines are for a fluid with an extremely large magnetic diffusivity. The dashed lines equivalently represent the cases in which the magnetic field is allowed to become well-established before any changes in the pressure gradient. Thus, it appears that if a large magnetic field experiences a delay in penetrating the fluid during the transient, damped flow oscillations will occur. If these oscillations are to be avoided, it is only necessary to establish the magnetic field before changing the pressure gradient.

Similar, but less pronounced, oscillations occur in the temperature-difference function as shown in Figure 4. Increasing the Hartmann number is also observed to decrease the temperature difference between the fluid and the wall.

Finally, the transient Nusselt number is shown in Figure 5. A decrease in the Nusselt number is noted as the Hartmann number increases, an undershoot occurring at M = 20, and oscillations at M = 50. In fact, the Nusselt number drops to about 65% of the steady value at M = 50. These oscillations do not occur if $Pr/Pr_m \gg 1$ or if the magnetic field is established before the pressure gradient is changed.

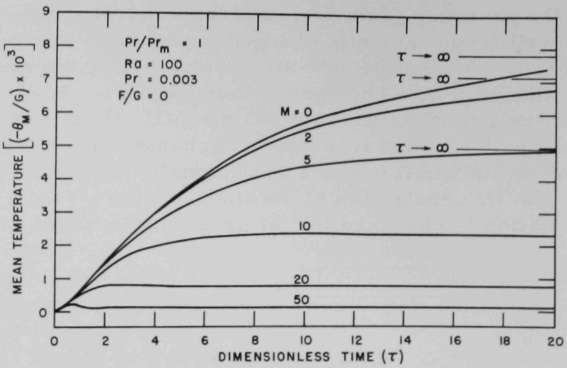

112-4418

Fig. 4

Effect of Hartmann Number on Transient Mean Temperature Difference

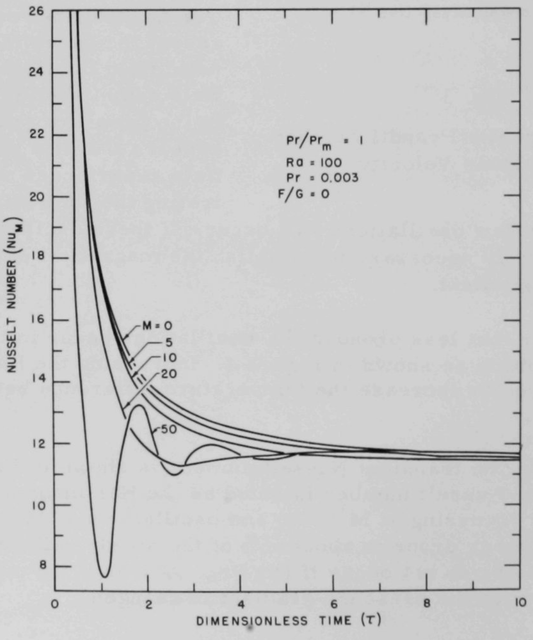

Fig. 5

Effect of Hartmann Number on Transient Nusselt Number

Effect of the Rayleigh Number

Figures 6, 7, and 8 show the effect of the Rayleigh number (a measure of free convection) upon the mean velocity, temperature, and Nusselt number, respectively. The curve labeled Ra = 0 in Figure 6 represents the following situation: The fluid is initially at rest and a very small magnetic field is established; at zero time, the pressure gradient is suddenly increased and the fluid is put into motion, and the steady-state velocity is approached asymptotically. The curves labeled Ra = 10, 10^2, 10^3, and 10^4 represent the same situation except that the wall temperature (or wall heat flux) is also suddenly increased at zero time. Increased free-convection effects (larger Ra) decrease the mean velocity, and at sufficiently large values of Ra, some oscillation occurs.

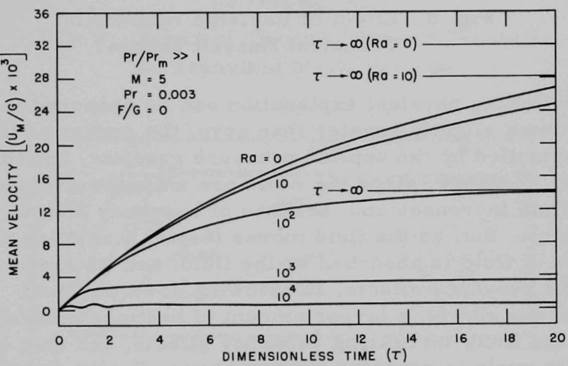

Fig. 6. Effect of Rayleigh Number on Transient Mean Velocity

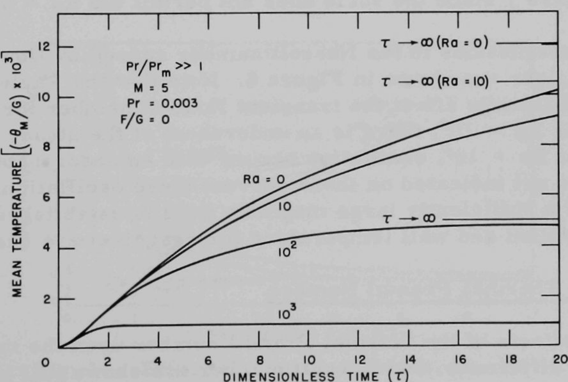

Fig. 7. Effect of Rayleigh Number on Transient Mean Temperature Difference

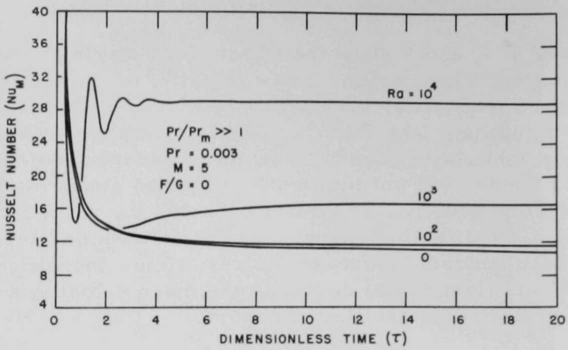

Fig. 8. Effect of Rayleigh Number on Transient Nusselt Number

The following physical explanation can be proposed for this oscillation: For times slightly greater than zero, the motion of the fluid is primarily controlled by the applied pressure gradient, and the fluid starts to accelerate. However, since the walls are uniformly heated, the temperature of the fluid increases and, because of buoyancy effects, the fluid accelerates faster. But, as the fluid moves faster, a smaller amount of heat per unit mass of fluid is absorbed by the fluid, and its temperature drops, decreasing the buoyancy effects, and slowing down the fluid. Now, as the fluid moves more slowly, a larger amount of heat per unit mass of fluid is absorbed by the fluid, increasing buoyancy effects, and thus increasing the velocity. This cycle is repeated over and over, finally damped by the thermal diffusivity of the fluid, and a steady-state condition is attained. The aforementioned oscillations in the temperature difference are not shown in Figure 7 since the scale does not permit the Ra = 10^4 curve to fit.

The oscillations in the Nusselt number caused by flow and temperature oscillations are shown in Figure 8. Note that the Rayleigh number does not significantly affect the transient Nusselt number for values of Ra $< 10^2$. For Ra = 10^3, there is an undershoot of the steady value of Nu_M by 23%, and at Ra = 10^4, oscillation occurs with an undershoot of 52%. Although it is not indicated on these curves, these oscillations could be eliminated if a sufficiently large magnetic field is established before the pressure gradient and wall temperature (or heat flux) are changed.

Effect of the Thermal Prandtl Number

The effects of the thermal Prandtl number upon the mean velocity, temperature difference, and Nusselt number are shown in Figures 9, 10, and 11, respectively. The curves represent the following case: Initially

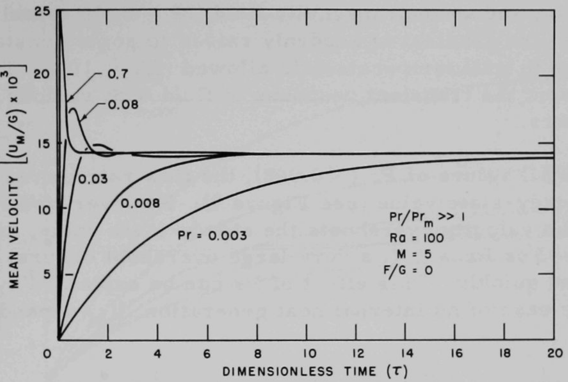

Fig. 9. Effect of Thermal Prandtl Number on Transient Mean Velocity

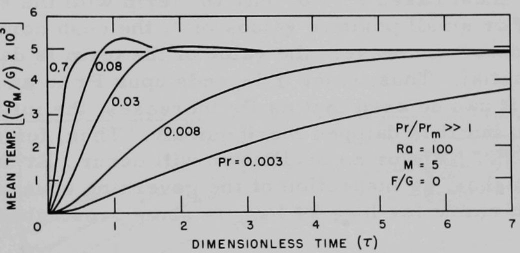

Fig. 10. Effect of Thermal Prandtl Number on Transient Temperature Difference

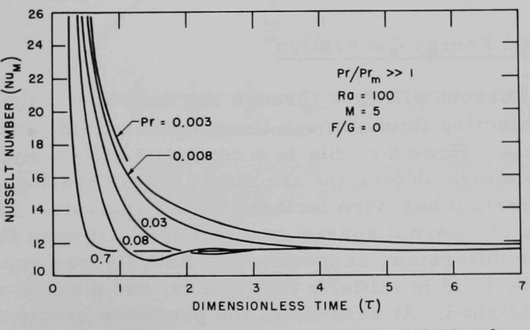

Fig. 11. Effect of Thermal Prandtl Number on Transient Nusselt Number

there is no flow, and a small magnetic field (M = 5) is established. At zero time, the pressure gradient is suddenly raised to some constant value and a small change in wall temperature is allowed (Ra = 100). The family of curves represent the transient response of fluid with various thermal Prandtl numbers.

For small values of Pr (<0.008), the flow rate increases monotonically to its steady-state value (see Figure 9). However, for Pr greater than about 0.030, the velocity overshoots the steady-state value, and some oscillation occurs. For Pr = 0.7, a very large overshoot occurs, but steady flow is reached quickly. This effect of Pr can be explained by the equations for U_M; in the case of no internal heat generation, U_M depends primarily on terms like

$$\exp\left[-\frac{\tau}{2}\left(\frac{m\pi}{2}\right)^2 (1 + Pr)\right] \cosh\left(\frac{1}{2}\gamma\tau\right) \text{ and } \exp\left[-\frac{\tau}{2}\left(\frac{m\pi}{2}\right)^2 (1 + Pr)\right] \cos\left(\frac{\tau}{2}\sqrt{-\gamma^2}\right).$$

Thus, since for most cases $\gamma^2 > 0$, only the term with the hyperbolic cosine is discussed. For small positive values of τ, the cosh dominates the value of the term, and as τ increases, the value of the term is damped by the negative exponential. Thus, since γ depends upon Pr in an approximately linear fashion, it can be seen that as Pr increases, the initial rise of this term increases, but it is damped more quickly. Thus, for sufficiently large values of Pr, little or no oscillation will occur. At infinite time, the effect of Pr vanishes, as inspection of the governing equations (14), (15), and (16) can determine (as long as Pr_m is some prescribed multiple of Pr).

The only significant effect of the thermal Prandtl number upon the temperature difference and Nusselt number, as shown in Figures 10 and 11, is that the time required to reach steady state is increased as Pr is decreased. Only a slight oscillation is noted at Pr = 0.08.

Effect of Internal Energy Generation

Since a current will flow through the fluid due to the motion of the electrically conducting fluid through the magnetic field, internal electrical heating will occur. However, this is a nonlinear effect, and for simplicity as well as to generally determine the effect of this heating, a uniform internal heat generation has been included in the analysis. Figures 12 and 13 show the effects of internal energy generation (F/G) upon the mean velocity and temperature difference, respectively. Both figures represent the following case: The fluid is initially motionless, and a small magnetic field (M = 5) is established. At zero time, the pressure gradient is suddenly increased, and the fluid starts to generate heat at a constant rate of F/G. (The wall temperature is also changed slightly.)

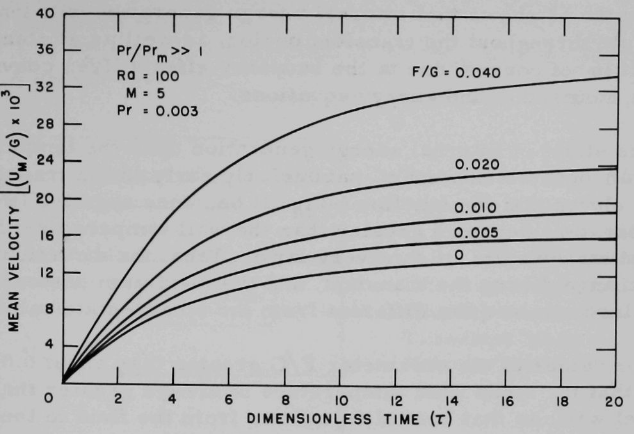

Fig. 12. Effect of Internal Energy Generation on Transient Mean Velocity

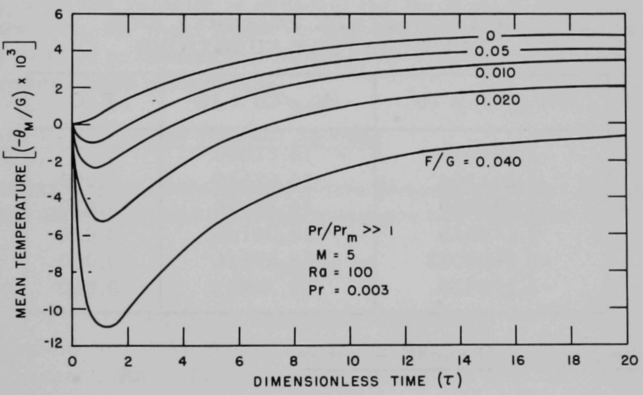

Fig. 13. Effect of Internal Energy Generation on Transient Mean Temperature Difference

Figure 12 shows that internal energy generation will tend to increase the flow rate throughout the transient period, as well as at steady state. This effect is, of course, due to the buoyancy effects (free convection) that couple the momentum and energy equations.

The effect of internal energy generation upon the temperature difference can become important, particularly early in the transient period. Figure 13 shows that the function $(-\theta_M/G)$ becomes negative (the mean fluid temperature becomes greater than the wall temperature) for $\tau > 0$, although at steady state, it can be positive. Thus, the direction of heat flow can change during the transient, and the maximum unsteady temperatures attained can be quite different from the steady-state values.

For values of the parameter F/G greater than about 0.036*, it is observed that the mean fluid temperature is always greater than that of the channel wall, so that heat always flows from the fluid to the wall.

The steady-state mean velocity and temperature difference functions are shown in Table I for M = 5, Ra = 100, and Pr = 0.003.

Table I

STEADY-STATE VELOCITY AND TEMPERATURE FUNCTIONS

$(-\theta_M/G) \times 10^3$	$(U_M/G) \times 10^3$	F/G
4.916978	14.21840	0
4.231264	16.67689	0.005
3.545549	19.13538	0.010
2.174325	24.04146	0.020
-0.5683022	33.87536	0.040
-3.310929	43.70927	0.060

Effect of the Magnetic Prandtl Number

As indicated in Figure 3 and discussed previously, flow oscillations can occur when the magnetic diffusivity is small. This section will investigate the overall effect of the magnetic diffusivity (as measured by Pr/Pr_m) upon the flow and heat transfer and determine how large Pr/Pr_m must be for the solutions obtained for $Pr/Pr_m \gg 1$ to be valid.

Equations (10), (11), and (12) were solved using the analysis described in Appendix B for arbitrary values of Pr/Pr_m, and using step-changes in the pressure gradient and wall temperature. The results are

*By interpolation of the data in Table I.

shown in Figure 14. For convenience in the interpretation of the results, the ratio of the mean velocity at an arbitrary value of Pr/Pr_m to that at $Pr/Pr_m = 1$ is presented as a function of Pr/Pr_m with the Hartmann number as a parameter.

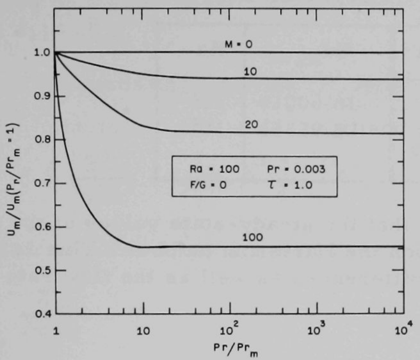

Fig. 14

Effect of Magnetic Prandtl Number on Transient Mean Velocity Ratio

For large values of M (liquid-metal MHD generators normally operate at values of M near 100 to 500), the effect of Pr/Pr_m is limited to values of Pr/Pr_m less than approximately 10. However, the total effect of Pr/Pr_m upon the velocity is greatest for the largest values of M. The values of Pr/Pr_m for most liquid metals are greater than 1000 (Table B1), so that the results presented for $Pr/Pr_m \gg 1$ can be used with confidence for liquid-metal MHD generators.

<u>Steady-state Values of the Nusselt Number</u>

Several values of the steady-state Nusselt numbers for various values of the Hartmann and Rayleigh numbers are shown in Tables II and III.

Table II

STEADY-STATE VALUES OF THE NUSSELT NUMBER FOR Ra = 100, Pr = 0.003, AND F = 0

$Nu_{M,ss}$	M	$Nu_{M,ss}$	M
11.76325	0	11.60041	20
11.70922	2	11.74976	50
11.56678	5	11.80548	100
11.51479	10		

Table III

STEADY-STATE VALUES OF THE NUSSELT NUMBER FOR $M = 5$, $Pr = 0.003$, AND $F = 0$

$Nu_{M,ss}$	Ra	$Nu_{M,ss}$	Ra
10.60981	0	16.60019	10^3
10.51462	10	28.98351	10^4
11.56678	10^2		

It is somewhat surprising that the steady-state values of the Nusselt number do not depend strongly upon the Hartmann number. This is due to the decrease of the temperature differences as well as the flow rate with increases in M.

SUMMARY AND CONCLUSIONS

The effects of combined forced and free convection, a transverse magnetic field, internal energy generation, and fluid diffusive properties upon the unsteady, fully-developed, laminar flow of an electrically conducting fluid through a vertical parallel-plate channel has been analytically studied. An oscillatory approach to steady state occurs whenever the Hartmann or Rayleigh numbers are large, or the thermal Prandtl number is near unity. Conversely, the oscillations are largely damped by the diffusive character of the fluid, i.e., for very small or very large thermal or magnetic Prandtl numbers. Also, if a sufficiently large magnetic field is allowed to become established before the fluid is put in motion, little, if any, oscillation is observed.

Unsteady fluid temperatures were found to be significantly different from the steady-state values for some ranges of the parameters, so that any design of an MHD device must take cognizance of the start-up phenomena to prevent any untoward occurrence, e.g., overheating of channel walls or boiling of the liquid. Also, it is conceivable that electrical overloading could occur due to large-scale flow oscillations in certain cases.

APPENDIX A

Specialized Temperature Field

For an unsteady, fully developed flow to exist, restrictions must be placed on the temperature field. These restrictions will be determined in this appendix.

Differentiating equation (6), first with respect to x and then y, results in

$$0 = \frac{\partial^3 p}{\partial y \partial x^2} + \rho_R g \beta \frac{\partial^2 (T - T_R)}{\partial y \partial x}, \qquad \text{(A1)}$$

and differentiation of equation (7) twice with respect to x yields

$$\frac{\partial^3 p}{\partial x^2 dy} = 0. \qquad \text{(A2)}$$

The condition on $(T - T_R)$ for a fully developed unsteady flow is then

$$\frac{\partial^2 (T - T_R)}{\partial y \partial x} = 0, \qquad \text{(A3)}$$

or, if T_R is taken as the wall temperature, $T_R = T_W(x,t)$, the criterion (A3) becomes

$$\frac{\partial^2 T}{\partial y \partial x} = 0, \qquad \text{(A3a)}$$

so that $T(x,y,t) = f_1(x,t) + f_2(y,t)$. If the reasoning as used in Reference 12 is followed, it is easily shown that $f_1(x,t) = Ax + f_3(t)$, so that

$$T(x,y,t) = Ax + f_3(t) + f_2(y,t). \qquad \text{(A4)}$$

Now, since $T - T_R = T - T_W = f_2(y,t) - f_2(a,t)$ is a function of y and t only, $T - T_W$ can be substituted into equation (6), resulting in

$$\frac{\partial u}{\partial t} - \nu_R \frac{\partial^2 u}{\partial y^2} - \frac{B_0}{\rho_R \mu_0} \frac{\partial B_x}{\partial y} - g\beta(T - T_W) = -\frac{1}{\rho_R} \frac{\partial \rho}{\partial x} - g. \qquad \text{(A5)}$$

The left-hand side of equation (A5) is a function of y and t only; thus, the right-hand side can at most be a function of y and t also. Hence, let

$$-\frac{1}{\rho_R} \frac{\partial \rho}{\partial x} - g = f_4(y,t). \qquad \text{(A6)}$$

But, if equation (A6) is differentiated with respect to y, and it is noted that $\partial^2 \rho/\partial y \partial x = 0$ [from equation (7)], then, $\partial f_4/\partial y = 0$, so that $f_4(y,t) = S(t)$, where S(t) is a prescribed function.

Finally, the momentum and energy equations can be written as follows, noting the preceding arguments:

$$\frac{\partial u}{\partial t} = \nu_R \frac{\partial^2 u}{\partial y^2} + \frac{B_0}{\rho_R \mu_0} \frac{\partial B_x}{\partial y} + g\beta(T - T_W) + S(t); \tag{6a}$$

$$\frac{\partial T}{\partial t} + Au = \alpha_R \frac{\partial^2 T}{\partial y^2} + \frac{Q}{\rho_R c_R}. \tag{8a}$$

The above two equations, in conjunction with equation (5), constitute a description of unsteady, fully developed, convective, magnetohydrodynamic flow.

APPENDIX B

Solutions of Equations (10), (11), and (12)

The system of equations (10), (11), and (12), with the conditions (13) and (14), can be reduced to an ordinary differential system by expanding the dependent variables in Fourier series.

$$U(Y,\tau) = \sum_{m=0}^{\infty} U_m(\tau) \sin \frac{m\pi}{2} (Y+1),$$

$$\theta(Y,\tau) = \sum_{m=0}^{\infty} \theta_m(\tau) \sin \frac{m\pi}{2} (Y+1), \tag{B1}$$

and

$$B(Y,\tau) = \sum_{m=0}^{\infty} B_m(\tau) \cos \frac{m\pi}{2} (Y+1).$$

By direct substitution, there results

$$\frac{dB_m}{d\tau} + \left(\frac{m\pi}{2}\right)^2 (Pr/Pr_m) B_m = \left(\frac{m\pi}{2}\right) U_m, \tag{B2}$$

$$\frac{1}{Pr}\frac{dU_m}{dt} + \left(\frac{m\pi}{2}\right)^2 U_m = Ra\theta_m - \left(\frac{m\pi}{2}\right)\left(\frac{M^2 Pr}{Pr_m}\right) B_m + G_m(\tau), \tag{B3}$$

and

$$\frac{d\theta_m}{d\tau} + \left(\frac{m\pi}{2}\right)^2 \theta_m = -U_m + F_m(\tau) - H_m(\tau), \tag{B4}$$

with the initial conditions

$$U_m(0) = U_{mi},$$

$$B_m(0) = B_{mi}, \tag{B5}$$

and

$$\theta_m(0) = \theta_{mi},$$

where

$$\phi_m = \int_{-1}^{+1} \phi(Y) \sin \frac{m\pi}{2} (Y+1) dY \tag{B6}$$

for $\phi = U_i$, B_i, θ_i, and F, and where

$$\frac{G_m(\tau)}{G(\tau)} = \frac{H_m(\tau)}{H(\tau)} = \frac{2}{m\pi}(1 - \cos m\pi). \tag{B6a}$$

The set of equations (B2), (B3), and (B4) can now be operated on with the Laplace transform, resulting in

$$s\overline{B}_m - B_{mi} + \left(\frac{m\pi}{2}\right)^2 (Pr/Pr_m)\overline{B} = \left(\frac{m\pi}{2}\right)\overline{U}_m, \tag{B2a}$$

$$\frac{s}{Pr}\overline{U}_m - \frac{1}{Pr}U_{mi} + \left(\frac{m\pi}{2}\right)^2 \overline{U}_m = Ra\overline{\theta}_m - \left(\frac{m\pi}{2}\right)\left(\frac{M^2 Pr}{Pr_m}\right)\overline{B}_m + \overline{G}_m, \tag{B3a}$$

and

$$s\overline{\theta}_m - \theta_{mi} + \left(\frac{m\pi}{2}\right)^2 \overline{\theta}_m = -\overline{U}_m + \overline{F}_m - \overline{H}_m, \tag{B4a}$$

where

$$\overline{\phi} = \int_0^\infty e^{-st}\phi(\tau)d\tau. \tag{B7}$$

This linear, algebraic set of equations can be solved for $\overline{B}_m$, $\overline{U}_m$, and $\overline{\theta}_m$ to yield

$$\overline{B}_m = \left[B_{mi} + \left(\frac{m\pi}{2}\right)\overline{U}_m\right] \Big/ \left[s + \left(\frac{m\pi}{2}\right)^2 (Pr/Pr_m)\right], \tag{B8}$$

$$\overline{\theta}_m = (\theta_{mi} - \overline{U}_m + \overline{F}_m - \overline{H}_m) \Big/ \left[s + \left(\frac{m\pi}{2}\right)^2\right], \tag{B9}$$

and

$$\begin{aligned}\overline{U}_m = \Bigg\{&\left(\overline{G}_m + \frac{U_{mi}}{Pr}\right)\left[s + \left(\frac{m\pi}{2}\right)^2\right]\left[s + \left(\frac{m\pi}{2}\right)^2\left(\frac{Pr}{Pr_m}\right)\right] + Ra(\theta_{mi} + \overline{F}_m - \overline{H}_m)\left[s + \left(\frac{m\pi}{2}\right)^2\left(\frac{Pr}{Pr_m}\right)\right] \\ &- \left(\frac{m\pi}{2}\right)\left(\frac{M^2 Pr}{Pr_m}\right)\left[s + \left(\frac{m\pi}{2}\right)^2\right]\Bigg\}\Bigg\{\left[\frac{s}{Pr} + \left(\frac{m\pi}{2}\right)^2\right]\left[s + \left(\frac{m\pi}{2}\right)^2\right]\left[s + \left(\frac{m\pi}{2}\right)^2\left(\frac{Pr}{Pr_m}\right)\right] \\ &+ Ra\left[s + \left(\frac{m\pi}{2}\right)^2\left(\frac{Pr}{Pr_m}\right)\right] + \left(\frac{m\pi}{2}\right)^2\left(\frac{M^2 Pr}{Pr_m}\right)\left[s + \left(\frac{m\pi}{2}\right)^2\right]\Bigg\}^{-1}.\end{aligned} \tag{B10}$$

The general inverse transformation of equation (B10) is relatively straightforward. However, it presents a difficult computational problem due to the complexity of the denominator and its roots. Thus, to substantially reduce the numerical work, the inverse transform will be accomplished only for two values of the ratio Pr/Pr_m, which may be rewritten as ν_m/α. Using these two expressions, the effects of all other parameters will be investigated. Then, fixing all of the parameters except M and Pr/Pr_m, equation (B10) will be directly transformed, and the effect of Pr/Pr_m will be studied.

Case of $Pr = Pr_m$

If the thermal and magnetic diffusivities of the fluid are equal, equation (B10) can be considerably simplified due to the equality of Pr and Pr_m. Thus,

$$\overline{U}_m = \frac{(U_{mi} + Pr\overline{G}_m)\left[s + \left(\frac{m\pi}{2}\right)^2\right] + RaPr(\theta_{mi} + \overline{F}_m - \overline{H}_m) - \left(\frac{m\pi}{2}\right)M^2PrB_{mi}}{\left[s + \left(\frac{m\pi}{2}\right)^2 Pr\right]\left[s + \left(\frac{m\pi}{2}\right)^2\right] + RaPr + \left(\frac{m\pi}{2}\right)^2 M^2Pr}. \tag{B10a}$$

The inverse transform of equation (B10a) can now be easily obtained as

$$\begin{aligned} U_m(\tau) = {} & \frac{U_{mi}}{s_1 - s_2}\left\{\left[s_1 + \left(\frac{m\pi}{2}\right)^2\right]e^{s_1\tau} - \left[s_2 + \left(\frac{m\pi}{2}\right)^2\right]e^{s_2\tau}\right\} \\ & + \left[\frac{RaPr\theta_{mi} - \left(\frac{m\pi}{2}\right)M^2PrB_{mi}}{s_1 - s_2}\right]\left(e^{s_1\tau} - e^{s_2\tau}\right) \\ & + \left[\frac{PrG_m(\tau)}{s_1 - s_2}\right] * \left\{\left[s_1 + \left(\frac{m\pi}{2}\right)^2\right]e^{s_1\tau} - \left[s_2 + \left(\frac{m\pi}{2}\right)^2\right]e^{s_2\tau}\right\} \\ & + \left(\frac{RaPr}{s_1 - s_2}\right)\left[F_m(\tau) - H_m(\tau)\right] * \left(e^{s_1\tau} - e^{s_2\tau}\right), \end{aligned} \tag{B11}$$

where

$$\left.\begin{matrix} s_1 \\ s_2 \end{matrix}\right\} = -\frac{m^2\pi^2}{8}(1 + Pr) \pm \frac{1}{2}\left[\left(\frac{m\pi}{2}\right)^4(1 - Pr)^2 - 4\left(\frac{m\pi}{2}\right)^2 M^2Pr - 4RaPr\right]^{1/2}, \tag{B12}$$

and

$$\phi_1(\tau) * \phi_2(\tau) = \int_0^\tau \phi_1(\tau - t)\phi_2(t)dt. \tag{B13}$$

From equations (B8) and (B9), the following expressions for $B_m(\tau)$ and $\theta_m(\tau)$ can directly be obtained in terms of $U_m(\tau)$:

$$B_m(\tau) = B_{mi}\, e^{-\left(\frac{m\pi}{2}\right)^2 \tau} + \left(\frac{m\pi}{2}\right) U_m(\tau) * e^{-\left(\frac{m\pi}{2}\right)^2 \tau}, \tag{B14}$$

and

$$\theta_m(\tau) = \theta_{mi}\, e^{-\left(\frac{m\pi}{2}\right)^2 \tau} - \left[U_m(\tau) - F_m(\tau) + H_m(\tau)\right] * e^{-\left(\frac{m\pi}{2}\right)^2 \tau}. \tag{B15}$$

The functions $U(Y,\tau)$, $B(Y,\tau)$, and $\theta(Y,\tau)$ can now be determined by using equations (B1).

Case of $Pr \gg Pr_m$

If the thermal and magnetic diffusivities of conducting liquids are examined, it is found that ν_m is usually much larger than α. For sodium at 1300°F, $\nu_m/\alpha = Pr/Pr_m \approx 930$, while other liquids have even larger values. Table Bl indicates the value of the ratio Pr/Pr_m for several of the more common liquid metals and other liquids.

Table Bl

VALUES OF THE RATIO Pr/Pr_m

Liquid	Temperature (°F)	Pr/Pr_m
Mercury	700	9.8×10^4
Cesium	100	5.2×10^3
Potassium	800	1.3×10^3
Rubidium	800	3.1×10^3
NaK (78%K)	600	8.4×10^3
Lithium	400	1.0×10^4
H_2SO_4 (concentrated solution)	68	$\sim 10^{11}$
NaCl (37% solution)	68	$\sim 3 \times 10^{11}$

Table Bl indicates that the assumption of $Pr \gg Pr_m$ should be valid for many liquids that are of interest in magnetohydrodynamic devices. Thus, if Pr/Pr_m is formally allowed to approach infinity in equations (B8) through (B10), an approximate expression for the velocity, temperature, and magnetic fields can be obtained.

From equation (B10), it can be shown that as (Pr/Pr_m) approaches infinity,

$$\lim_{\left(\frac{Pr}{Pr_m}\right)\to\infty} \bar{U}_m = \frac{\left(\bar{G}_m + \frac{U_{mi}}{Pr}\right)\left[s + \left(\frac{m\pi}{2}\right)^2\right] + Ra(\theta_{mi} + \bar{F}_m - \bar{H}_m) - (2M^2B_{mi}/m\pi)\left[s + \left(\frac{m\pi}{2}\right)^2\right]}{\left[\frac{s}{Pr} + \left(\frac{m\pi}{2}\right)^2\right]\left[s + \left(\frac{m\pi}{2}\right)^2\right] + M^2\left[s + \left(\frac{m\pi}{2}\right)^2\right] + Ra} \tag{B10b}$$

The inverse Laplace transform of this expression can now be directly obtained, resulting in

$$U_m(\tau) = \left\{\frac{RaPr\theta_{mi} + \left[s_4 + \left(\frac{m\pi}{2}\right)^2\right]\left(U_{mi} - \frac{2M^2PrB_{mi}}{m\pi}\right)}{s_4 - s_5}\right\}e^{s_4\tau}$$

$$+ \left\{\frac{PrG_m(\tau)\left[s_4 + \left(\frac{m\pi}{2}\right)^2\right] + RaPr\left[F_m(\tau) - H_m(\tau)\right]}{s_4 - s_5}\right\} * e^{s_4\tau}$$

$$- \left\{\frac{RaPr\theta_{mi} + \left[s_5 + \left(\frac{m\pi}{2}\right)^2\right]\left(U_{mi} - \frac{2M^2PrB_{mi}}{m\pi}\right)}{s_4 - s_5}\right\}e^{s_5\tau}$$

$$- \left\{\frac{PrG_m(\tau)\left[s_5 + \left(\frac{m\pi}{2}\right)^2\right] + RaPr\left[F_m(\tau) - H_m(\tau)\right]}{s_4 - s_5}\right\} * e^{s_5\tau}, \tag{B16}$$

where

$$\left.\begin{matrix} s_4 \\ s_5 \end{matrix}\right\} = -\left(\frac{m^2\pi^2}{8}\right)(1 + Pr) - \frac{M^2Pr}{2} \pm \frac{1}{2}\left[\left(\frac{m\pi}{2}\right)^4(1 - Pr)^2 - 2PrM^2\left(\frac{m\pi}{2}\right)^2(1 - Pr)\right.$$

$$\left. + M^4Pr^2 - 4PrRa\right]^{1/2}, \tag{B17}$$

and the convolution integral is defined in equation (B13).

Letting (Pr/Pr_m) approach infinity in equations (B8) and (B9) shows that $\bar{B}_m$ approaches zero, and $\bar{\theta}_m = (\theta_{mi} - \bar{U}_m + \bar{F}_m - \bar{H}_m)/\left[s + \left(\frac{m\pi}{2}\right)^2\right]$ is unchanged. Thus, $\theta_m(\tau)$ can be determined by using the relation (B15) and the result for $U_m(\tau)$ in (B16). Finally, the functions $U(Y,\tau)$, $\theta(Y,\tau)$ can be obtained by using equations (B1).

The assumption that the magnetic diffusivity is much larger than the thermal diffusivity is tantamount to neglecting the induced magnetic field in equations (5) through (8). Thus, the applied magnetic field passes through the fluid with only a negligible distortion.

Case of Arbitrary Pr/Pr_m

To solve equations (B8) through (B10) for arbitrary values of Pr/Pr_m, the only problem is the inverse transformation of equation (B10). The first step is the calculation of the zeros of the denominator of equation (B10); let these three zeros be called s_1, s_2, and s_3 (these numbers, in general, will be complex). Then, the expression for $\overline{U}_m$ may be rewritten as

$$\overline{U}_m = \frac{A_1(s)}{s - s_1} + \frac{A_2(s)}{s - s_2} + \frac{A_3(s)}{s - s_3}, \tag{B18}$$

where

$$\frac{s_4 A_1(s)}{s_2 - s_3} = s_1\left[\left(\frac{m\pi}{2}\right)^2\left(1 + \frac{Pr}{Pr_m}\right)\left(\overline{G}_m + \frac{U_{mi}}{Pr}\right) + Ra\left(\theta_{mi} + \overline{F}_m - \overline{H}_m\right) - \left(\frac{m\pi}{2}\right) M^2 Pr B_{mi}/Pr_m\right]$$
$$+ s_1^2\left(\overline{G}_m + \frac{U_{mi}}{Pr}\right) + \left(\frac{m\pi}{2}\right)^2\left(\frac{Pr}{Pr_m}\right)\left[\left(\frac{m\pi}{2}\right)^2\left(\overline{G}_m + \frac{U_{mi}}{Pr}\right) + Ra\left(\theta_{mi} + \overline{F}_m - \overline{H}_m\right)\right] - \left(\frac{m\pi}{2}\right)^3 \frac{M^2 Pr B_{mi}}{Pr_m}, \tag{B19}$$

$$\frac{s_4 A_2(s)}{s_3 - s_1} = s_2\left[\left(\frac{m\pi}{2}\right)^2\left(1 + \frac{Pr}{Pr_m}\right)\left(\overline{G}_m + \frac{U_{mi}}{Pr}\right) + Ra\left(\theta_{mi} + \overline{F}_m - \overline{H}_m\right) - \left(\frac{m\pi}{2}\right) M^2 Pr B_{mi}/Pr_m\right]$$
$$+ s_2^2\left(\overline{G}_m + \frac{U_{mi}}{Pr}\right) + \left(\frac{m\pi}{2}\right)^2\left(\frac{Pr}{Pr_m}\right)\left[\left(\frac{m\pi}{2}\right)^2\left(\overline{G}_m + \frac{U_{mi}}{Pr}\right) + Ra\left(\theta_{mi} + \overline{F}_m - \overline{H}_m\right)\right] - \left(\frac{m\pi}{2}\right)^3 \frac{M^2 Pr B_{mi}}{Pr_m}, \tag{B20}$$

$$\frac{s_4 A_3(s)}{s_1 - s_2} = s_3\left[\left(\frac{m\pi}{2}\right)^2\left(1 + \frac{Pr}{Pr_m}\right)\left(\overline{G}_m + \frac{U_{mi}}{Pr}\right) + Ra\left(\theta_{mi} + \overline{F}_m - \overline{H}_m\right) - \left(\frac{m\pi}{2}\right) M^2 Pr B_{mi}/Pr_m\right]$$
$$+ s_3^2\left(\overline{G}_m + \frac{U_{mi}}{Pr}\right) + \left(\frac{m\pi}{2}\right)^2\left(\frac{Pr}{Pr_m}\right)\left[\left(\frac{m\pi}{2}\right)^2\left(G_{mi} + \frac{U_{mi}}{Pr}\right) + Ra\left(\theta_{mi} + \overline{F}_m - \overline{H}_m\right)\right] - \left(\frac{m\pi}{2}\right)^3 \frac{M^2 Pr B_{mi}}{Pr_m}, \tag{B21}$$

and

$$s_4 = s_1^2(s_2 - s_3) + s_2^2(s_3 - s_1) + s_3^2(s_1 - s_2). \tag{B22}$$

Now,

$$U_m(\tau) = A_1(\tau) * e^{s_1\tau} + A_2(\tau) * e^{s_2\tau} + A_3(\tau) * e^{s_3\tau}. \tag{B23}$$

Similarly

$$\theta_m(\tau) = e^{-\left(\frac{m\pi}{2}\right)^2\tau}\int_0^{\tau} e^{\left(\frac{m\pi}{2}\right)^2 t}\left[\theta_{mi} - U_m + F_m - H_m\right]dt, \tag{B24}$$

and

$$B_m(\tau) = e^{-\left(\frac{m\pi}{2}\right)^2(Pr/Pr_m)\tau}\int_0^{\tau} e^{\left(\frac{m\pi}{2}\right)^2(Pr/Pr_m)t}\left[B_{mi} + \left(\frac{m\pi}{2}\right)U_m\right]dt. \tag{B25}$$

APPENDIX C

Definitions of the Functions $\psi_1(m,\tau)$

$Pr/Pr_m = 1$

$$\psi_1(m,\tau) = \left(\frac{m\pi}{2}\right)^2 - e^{-A_1\tau}\left\{\left(\frac{m\pi}{2}\right)^2 \cos\left(\frac{\tau}{2}\sqrt{-\gamma^2}\right) + \left[\frac{\left(\frac{m\pi}{2}\right)^4 (1 - Pr) - 2Pr\left(\frac{M^2m^2\pi^2}{4}\right) + Ra)}{\sqrt{-\gamma^2}}\right]\sin\left(\frac{\tau}{2}\sqrt{-\gamma^2}\right)\right\}. \tag{C1}$$

$$\psi_2(m,\tau) = 1 - e^{-A_1\tau}\left[\cos\left(\frac{\tau}{2}\sqrt{-\gamma^2}\right) + \left(\frac{m\pi}{2}\right)^2\left(\frac{1+Pr}{\sqrt{-\gamma^2}}\right)\sin\left(\frac{\tau}{2}\sqrt{-\gamma^2}\right)\right]. \tag{C2}$$

$$\psi_3(m_0,\tau) = \frac{16PrG_m}{m_0^2\pi^2(1+Pr)^2}\left\{1 - \left[1 + \frac{m_0^2\pi^2}{16}(1 - Pr^2)\right]\exp\left[-\frac{\tau}{2}\left(\frac{m_0\pi}{2}\right)^2(1+Pr)\right]\right\}$$
$$+ \frac{64RaPrF_m}{m_0^4\pi^4(1+Pr)^2}\left\{1 - \left[1 + \frac{m_0^2\pi^2\tau}{8}(1+Pr)\right]\exp\left[-\frac{\tau}{2}\left(\frac{m_0\pi}{2}\right)^2(1+Pr)\right]\right\}. \tag{C3}$$

$$\psi_4(m,\tau) = \left(\frac{m\pi}{2}\right)^2 - e^{-A_1\tau}\left\{\left(\frac{m\pi}{2}\right)^2\cosh\left(\frac{1}{2}\gamma\tau\right) + \frac{1}{\gamma}\left[\left(\frac{m\pi}{2}\right)^4(1 - Pr) - 2Pr\left(Ra + \frac{M^2m^2\pi^2}{4}\right)\right]\sinh\left(\frac{1}{2}\gamma\tau\right)\right\}. \tag{C4}$$

$$\psi_5(m,\tau) = 1 - e^{-A_1\tau}\left[\cosh\left(\frac{1}{2}\gamma\tau\right) + \left(\frac{m\pi}{2}\right)^2\left(\frac{1+Pr}{\gamma}\right)\sinh\left(\frac{1}{2}\gamma\tau\right)\right]. \tag{C5}$$

$_6(m,\ ) = \frac{2}{m}$

$$\psi_6(m,\tau) = \left(\frac{2}{m\pi}\right)^2 - \left\{\frac{\left(\frac{m\pi}{2}\right)^4 + M^2\left(\frac{m\pi}{2}\right)^2 + Ra}{\left(\frac{m\pi}{2}\right)^2\left[M^2\left(\frac{m\pi}{2}\right)^2 + Ra\right]}\right\}e^{-\left(\frac{m\pi}{2}\right)^2\tau} + e^{-A_1\tau}\left\{\left[\frac{\left(\frac{m\pi}{2}\right)^2}{M^2\left(\frac{m\pi}{2}\right)^2 + Ra}\right]\cos\left(\frac{\tau}{2}\sqrt{-\gamma^2}\right)\right.$$
$$\left. - \left[\frac{\left(\frac{m\pi}{2}\right)^4(1 - Pr)}{\sqrt{-\gamma^2}\left(\frac{M^2m^2\pi^2}{4} + Ra\right)}\right]\sin\left(\frac{\tau}{2}\sqrt{-\gamma^2}\right)\right\}. \tag{C6}$$

$$\psi_7(m_0,\tau) = \frac{64PrG_m}{m_0^4\pi^4(1+Pr)^2}\left\{1 - \left[1 + \frac{\tau}{2}\left(\frac{m_0\pi}{2}\right)^2(1+Pr)\right]\exp\left[-\frac{\tau}{2}\left(\frac{m_0\pi}{2}\right)^2(1+Pr)\right]\right\}$$
$$+ \frac{256RaPrF_m}{m_0^6\pi^6(1+Pr)^2}\left\{1 - \left(\frac{1+Pr}{1-Pr}\right)^2\exp\left[-\left(\frac{m_0\pi}{2}\right)^2\tau\right]\right.$$
$$\left. + \left(\frac{2}{1 - Pr^2}\right)\left[2Pr - \frac{\tau}{2}\left(\frac{m_0\pi}{2}\right)^2(1 - Pr^2)\right]\exp\left[-\frac{\tau}{2}\left(\frac{m_0\pi}{2}\right)^2(1+Pr)\right]\right\}. \tag{C7}$$

$$\psi_8(m,\tau) = \left(\frac{2}{m\pi}\right)^2 - \left\{\frac{\left(\frac{m\pi}{2}\right)^4 + M^2\left(\frac{m\pi}{2}\right)^2 + Ra}{\left(\frac{m\pi}{2}\right)^2\left[M^2\left(\frac{m\pi}{2}\right)^2 + Ra\right]}\right\} \exp\left[-\left(\frac{m\pi}{2}\right)^2\tau\right] + e^{-A_1\tau}\left\{\left[\frac{\left(\frac{m\pi}{2}\right)^2}{M^2\left(\frac{m\pi}{2}\right) + Ra}\right]\cosh\left(\frac{1}{2}\gamma\tau\right)\right.$$

$$\left. - \left[\frac{\left(\frac{m\pi}{2}\right)^4(1 - Pr)}{\gamma\left(\frac{M^2m^2\pi^2}{4} + Ra\right)}\right]\sinh\left(\frac{1}{2}\gamma\tau\right)\right\}. \tag{C8}$$

$$\psi_9(m,\tau) = \psi_2(m,\tau),\ \psi_{10}(m,\tau) = \psi_6(m,\tau),\ \psi_{11}(m_0,\tau) = \psi_7(m_0,\tau),$$

$$\psi_{12}(m,\tau) = \psi_5(m,\tau),\ \psi_{13}(m,\tau) = \psi_8(m,\tau),\ A_1 = \frac{1}{2}\left(\frac{m\pi}{2}\right)^2(1 + Pr). \tag{C9}$$

$Pr/Pr_m >> 1$

$$\psi_1(m,\tau) = \left(\frac{m\pi}{2}\right)^2 - e^{A_2\tau}\left\{\left(\frac{m\pi}{2}\right)^2\cos\left(\frac{\tau}{2}\sqrt{-\gamma^2}\right) + \left[\frac{\left(\frac{m\pi}{2}\right)^4(1 - Pr) - Pr\left(\frac{M^2m^2\pi^2}{4} + 2Ra\right)}{\sqrt{-\gamma^2}}\right]\sin\left(\frac{\tau}{2}\sqrt{-\gamma^2}\right)\right\}. \tag{C10}$$

$$\psi_2(m,\tau) = 1 - e^{-A_2\tau}\left[\cos\left(\frac{\tau}{2}\sqrt{-\gamma^2}\right) + \left(\frac{2A_2}{\sqrt{-\gamma^2}}\right)\sin\left(\frac{\tau}{2}\sqrt{-\gamma^2}\right)\right]. \tag{C11}$$

$$\psi_3(m_0,\tau) = \frac{\left(\frac{m_0\pi}{2}\right)^2 PrG_m}{\left[\left(\frac{m_0^2\pi^2}{8}\right)(1 + Pr) + \frac{M^2Pr}{2}\right]^2}\left\{1 - \left[1 + \left(\frac{m_0^2\pi^2}{4} - \frac{m_0^2\pi^2 Pr}{4} - 2M^2Pr^2\right.\right.\right.$$

$$\left.\left.\left. - \frac{4M^4Pr^2}{m_0^2\pi^2}\right)\left(\frac{\tau}{4}\right)\right]e^{-A_2\tau}\right\} + \frac{RaPrF_m}{A_2^2}\left[1 - (1 + A_2\tau)e^{-A_2\tau}\right]. \tag{C12}$$

$$\psi_4(m,\tau) = \left(\frac{m\pi}{2}\right)^2 - e^{-A_2\tau}\left\{\left(\frac{m\pi}{2}\right)^2\cosh\left(\frac{1}{2}\gamma\tau\right) + \frac{1}{\gamma}\left[\left(\frac{m\pi}{2}\right)^4(1 - Pr) - Pr\left(\frac{M^2m^2\pi^2}{4} + 2Ra\right)\right]\sinh\left(\frac{1}{2}\gamma\tau\right)\right\}. \tag{C13}$$

$$\psi_5(m,\tau) = 1 - e^{-A_2\tau}\left[\left(\frac{2A_2}{\gamma}\right)\sinh\left(\frac{1}{2}\gamma\tau\right) + \cosh\left(\frac{1}{2}\gamma\tau\right)\right]. \tag{C14}$$

$$\psi_6(m,\tau) = \left(\frac{2}{m\pi}\right)^2 - \left[\frac{\left(\frac{m\pi}{2}\right)^4 + M^2\left(\frac{m\pi}{2}\right)^2 + Ra}{\left(\frac{m\pi}{2}\right)^2 Ra}\right] \exp\left[-\left(\frac{m\pi}{2}\right)^2\tau\right] + \frac{1}{Ra}\left[M^2 + \left(\frac{m\pi}{2}\right)^2\right] e^{-A_2\tau} \cos\left(\frac{\tau}{2}\sqrt{-\gamma^2}\right)$$

$$- \frac{e^{-A_2\tau}}{Ra\sqrt{-\gamma^2}}\left[\left(\frac{m\pi}{2}\right)^4(1 - Pr) + 2Ra + M^2\left(\frac{m\pi}{2}\right)^2(1 - 2Pr) - M^4 Pr\right] \sin\left(\frac{\tau}{2}\sqrt{-\gamma^2}\right). \quad \text{(C15)}$$

$$\psi_7(m_0,\tau) = \frac{G_m Pr}{A_2^2}\left[1 - (1 + A_2\tau)e^{-A_2\tau}\right] + \left(\frac{2}{A_2 m_0 \pi}\right)^2 Ra Pr F_m$$

$$\left\{1 - \left[\frac{\left(\frac{m_0\pi}{2}\right)^2(1 + Pr) + M^2 Pr}{\left(\frac{m_0\pi}{2}\right)^2(1 - Pr) - M^2 Pr}\right]^2 \exp\left[-\left(\frac{m_0\pi}{2}\right)^2\tau\right]\right\}$$

$$- \left[\frac{\left(\frac{m_0^2\pi^2}{2}\right) Pr\ e^{-A_2\tau}}{\left(\frac{m_0\pi}{2}\right)^2(1 - Pr) - M^2 Pr}\right]\left[\frac{2\left(M^2 + \frac{m_0^2\pi^2}{4}\right)}{\left(\frac{m_0\pi}{2}\right)^2(1 - Pr) - M^2 Pr} + A_2\tau\right]. \quad \text{(C16)}$$

$$\psi_8(m,\tau) = \left(\frac{2}{m\pi}\right)^2 - \left[\frac{\left(\frac{m\pi}{2}\right)^4 + M^2\left(\frac{m\pi}{2}\right)^2 + Ra}{Ra\left(\frac{m\pi}{2}\right)^2}\right] \exp\left[-\left(\frac{m\pi}{2}\right)^2\tau\right] + \frac{1}{Ra}\left[M^2 + \left(\frac{m\pi}{2}\right)^2\right] e^{-A_2\tau} \cosh\left(\frac{1}{2}\gamma\tau\right)$$

$$- \frac{e^{-A_2\tau}}{Ra\gamma}\left[\left(\frac{m\pi}{2}\right)^4(1 - Pr) + 2Ra + M^2\left(\frac{m\pi}{2}\right)^2(1 - 2Pr) - M^4 Pr\right] \sinh\left(\frac{1}{2}\gamma\tau\right). \quad \text{(C17)}$$

$$\psi_9(m,\tau) = \psi_{10}(m,\tau) = \psi_{11}(m_0,\tau) = \psi_{12}(m,\tau) = \psi_{13}(m,\tau) = 0;$$

$$A_2 = \left(\frac{m^2\pi^2}{8}\right)(1 + Pr) + \frac{1}{2} M^2 Pr. \quad \text{(C18)}$$

APPENDIX D

Mean Velocity and Temperature Difference Functions

The mean velocity and temperature difference functions as calculated from equations (26), (27), and (28) are

$$U_M(\tau) = \frac{1}{2}\int_{-1}^{+1} U(Y,\tau)dY = \sum_{\substack{\gamma^2<0 \\ \text{odd } m}} \left(\frac{2}{m\pi}\right)\left[\frac{G_m\psi_1(m,\tau) + RaF_m\psi_2(m,\tau)}{\left(\frac{m\pi}{2}\right)^4 + M^2\left(\frac{m\pi}{2}\right)^2 + Ra}\right]$$

$$+\left(\frac{1-\cos m_0\pi}{m_0\pi}\right)\psi_3(m_0,\tau) + \sum_{\substack{\gamma^2>0 \\ \text{odd } m}} \left(\frac{2}{m\pi}\right)\left[\frac{G_m\psi_4(m,\tau) + RaF_m\psi_5(m,\tau)}{\left(\frac{m\pi}{2}\right)^4 + M^2\left(\frac{m\pi}{2}\right)^2 + Ra}\right]; \qquad \text{(D1)}$$

$$-\theta_M(\tau) = -\frac{1}{2}\int_{-1}^{+1} \theta(Y,\tau)dY = \sum_{\substack{\gamma^2<0 \\ \text{odd } m}} \left(\frac{2}{m\pi}\right)\left[\frac{G_m\psi_2(m,\tau) + RaF_m\psi_6(m,\tau)}{\left(\frac{m\pi}{2}\right)^4 + M^2\left(\frac{m\pi}{2}\right)^2 + Ra}\right]$$

$$+\left(\frac{1-\cos m_0\pi}{m_0\pi}\right)\psi_7(m_0,\tau) + \sum_{\substack{\gamma^2>0 \\ \text{odd } m}} \left(\frac{2}{m\pi}\right)\left[\frac{G_m\psi_5(m,\tau) + RaF_m\psi_8(m,\tau)}{\left(\frac{m\pi}{2}\right)^4 + M^2\left(\frac{m\pi}{2}\right)^2 + Ra}\right]$$

$$-\sum_{\substack{m=1 \\ \text{odd } m}}^{\infty} \left(\frac{2}{m\pi}\right)^3 F_m\left[1 - e^{(-m\pi/2)^2\tau}\right]; \qquad \text{(D2)}$$

$$-\theta_{MM}(\tau) = \frac{-1}{2U_M(\tau)}\int_{-1}^{+1} U(Y,\tau)\theta(Y,\tau)dY = \sum_{\gamma^2<0}\left[\frac{G_m\psi_1 + RaF_m\psi_2}{\left(\frac{m\pi}{2}\right)^4 + M^2\left(\frac{m\pi}{2}\right)^2 + Ra}\right]$$

$$\left\{\frac{G_m\psi_2 + RaF_m\psi_6}{\left(\frac{m\pi}{2}\right)^4 + M^2\left(\frac{m\pi}{2}\right)^2 + Ra} - \frac{4F_m}{m^2\pi^2}\left[1 - e^{-(m\pi/2)^2\tau}\right]\right\}$$

$$+\psi_3(m_0,\tau)\left\{\psi_7(m_0,\tau) - \left[\frac{4F_{m_0}}{m_0^2\pi^2}\, 1 - e^{-(m_0\pi/2)^2\tau}\right]\right\}$$

$$+\sum_{\gamma^2>0}\left[\frac{G_m\psi_4 + RaF_m\psi_5}{\left(\frac{m\pi}{2}\right)^4 + M^2\left(\frac{m\pi}{2}\right)^2 + Ra}\right]\left\{\frac{G_m\psi_5 + RaF_m\psi_8}{\left(\frac{m\pi}{2}\right)^4 + M^2\left(\frac{m\pi}{2}\right)^2 + Ra} - \frac{4F_m}{m^2\pi^2}\left[1 - e^{-(m\pi/2)^2\tau}\right]\right\}. \qquad \text{(D3)}$$

ACKNOWLEDGMENT

The author wishes to express his appreciation to Mr. Allen Kennedy of the Applied Mathematics Division of Argonne National Laboratory for his work in the programing of an IBM 704 computer to perform the many calculations presented in this report.

REFERENCES

1. Hartmann, T., Kgl. Danske Videnskab. Selskab., Mat.-Fys. Medd. 15 (1937).
2. Shercliff, J. A., Proc. Cambridge Phil. Soc. 49 (1953), 136-144.
3. Shercliff, J. A., J. Fluid Mech. 1 (1956), 644-666.
4. Chang, C. C., and T. S. Lundgren, Proc. 1959 Heat Transf. Fluid Mech. Inst., 41-54.
5. Chekmarev, I. B., Soviet Phys. - Tech. Phys. 5 (1960), 313-319.
6. Yen, J. T., and C. C. Chang, Phys. Fluids 4 (1961), 1355-1361.
7. Tao, L. N., A.I.A.A. Journal 1 (1963), 461-462.
8. Ogawa, A., and Y. Sone, J. Phys. Soc. Jap. 16 (1961), 1423-1426.
9. Uflyand, Ya. S., Soviet Phys. - Tech. Phys. 6 (1962), 1031-1038.
10. Zeiberg, S. L., and W. K. Mueller, ASME Paper No. 61-SA-25 (1961).
11. Tao, L. N., J. Appl. Mech. 30 (1963), 257-262.
12. Cambel, A. B., Plasma Physics and Magnetofluidmechanics, McGraw-Hill Book Co., Inc., New York (1963).